IMPROVED HEATING AND COOLING IN TIGRESS SIMULATIONS

Munan Gong (龚慕南)[1]
Draft version May 24, 2019

ABSTRACT

Heating and cooling functions for the TIGRESS simulation (Kim & Ostriker 2017) based on equilibrium chemistry in Gong et al. (2017).

1. INTRODUCTION

The aim here is to develop physically motivated accurate heating and cooling functions for the TIGRESS simulation in different galactic environments.

The heating and cooling functions in this work take the hydro and radiation variables in the TIGRESS simulation and give the heating and cooling rates. The method here gives results similar to the equilibrium chemistry in the neutral and molecular ISM, but does not require solving the full chemistry ODEs. The abundances of different species are calculated (semi-)analytically from equilibrium conditions. The heating and cooling rates can be subsequently calculated from analytic expressions or interpolation tables (in the case of CO rotational lines). For hot gas ($T > 10^4$ K), we switch to collisional ionization equilibrium (CIE) cooling from tabulated cooling rates.

Section 2 gives a summary of the input and output parameters. Section 3 explains the calculation of the abundances of chemical species. Section 4 describes the heating and cooling processes included. Section 5 presents some tests for the heating and cooling functions. Finally, Section 6 lists some notes for the implementation in the Athena-TIGRESS code.

2. INPUT AND OUTPUT PARAMETERS

Table 1 list all the input parameters. The outputs are the heating rate Γ and cooling rate Λ:

$$\Gamma(x_i, T, Z, \xi_H, G_{\rm PE}, G_{\rm H_2}) = \Gamma_{\rm PE} + \Gamma_{\rm CR} + \Gamma_{\rm H_2pump}, \quad (1)$$

and

$$\begin{aligned}
&\Lambda(x_i, n, T, \langle|\mathrm{d}v/\mathrm{d}r|\rangle, Z, G_{\rm PE}) \\
&= \Lambda_{\rm Ly\alpha} + \Lambda_{\rm OI} + \Lambda_{\rm C^+} + \Lambda_{\rm CI} + \Lambda_{\rm CO} + \Lambda_{\rm rec}.
\end{aligned} \quad (2)$$

The relevant chemical abundances x_i are listed in Table 2, and can be calculated from the input parameters. The cooling rate from Equation (2) is appropriate for neutral and molecular ISM, which we identify as gas with $T \leq 10^4$ K. For $T \geq 10^{4.2}$ K, we switch to using tabulated CIE cooling for hot gas (Wiersma et al. 2009). To avoid discontinuity in the cooling rates, a log-linear interpolation between the cooling rate by Equation (2) at $T = 10^4$ K and the CIE cooling at $T = 10^{4.2}$ K is used for $10^{4.0}$ K $< T < 10^{4.2}$ K.

The details about these heating and cooling processes are explained in the following sections.

[1] Max-Planck Institute for Extraterrestrial Physics, Garching by Munich, 85748, Germany; munan@mpe.mpg.de

3. CHEMICAL ABUNDANCES

In order to calculate the heating and cooling rates in Equations (1) and (2), we need to know the chemical abundances of the species listed in Table 2. We explain the calculation of the abundances of these species below.

3.1. H_2 *Abundance*

The H_2 abundance can be obtained from Equation (18) in Gong et al. (2018):

$$x_H n k_{\rm gr} = 1.65 x_{\rm H_2} k_{\rm CR}. \quad (3)$$

The left hand side is the rate of H_2 formation on dust grains. On the right hand side, $x_{\rm H_2} k_{\rm CR}$ is the destruction of H_2 by cosmic rays, and the 1.65 factor comes from additional channels of H_2 destruction by H_2^+ and H_2 formation by H_3^+. If we take the photo-dissociation of H_2 by FUV radiation into account, which can be important at the edge of the cloud especially when the cosmic ray ionization rate is low, and the collisional dissociation of H_2, which can be important in shocks, then Equation (3) becomes:

$$\begin{aligned}
x_H n k_{\rm gr} =& 1.65 x_{\rm H_2} k_{\rm CR} + x_{\rm H_2} k_\gamma \\
&+ x_{\rm H_2} x_H n k_{\rm H_2,H} + x_{\rm H_2}^2 n k_{\rm H_2,H_2},
\end{aligned} \quad (4)$$

where $k_\gamma = 5.7 \times 10^{-11} G_{\rm H_2}$ s^{-1} is the photo-dissociation rate of H_2, and $k_{\rm H_2,H}$ and $k_{\rm H_2,H_2}$ are the collisional dissociation rates of H_2 by H and H_2, given in reactions 22 and 23 in Table 1 of Gong et al. (2017). Using $x_H = 1 - 2x_{\rm H_2}$ and $k_{\rm CR} = 2\xi_H(2.3x_{\rm H_2} + 1.5x_H)$, Equation (4) can be written as a quadratic equation for $x_{\rm H_2}$:

$$\begin{aligned}
&a x_{\rm H_2}^2 + b x_{\rm H_2} + c = 0 \\
&a = 2.31\xi_H + 2n k_{\rm H_2,H} - n k_{\rm H_2,H_2} \\
&b = -(4.95\xi_H + 2n k_{\rm gr} + k_\gamma + n k_{\rm H_2,H}), \\
&c = n k_{\rm gr},
\end{aligned} \quad (5)$$

and the H_2 abundance $x_{\rm H_2} = (-b - \sqrt{b^2 - 4ac})/(2a)$. If $k_\gamma = 0$, this recovers the result in Gong et al. (2018) without photo-dissociation.

3.2. C^+, H^+ *and* e^- *Abundances*

The C^+ equilibrium abundance is calculated from the balancing of the C^+ creation by cosmic-ray and FUV ionisation

$$\mathrm{cr} + \mathrm{C} \to \mathrm{C}^+ + \mathrm{e}$$

$$\gamma + \mathrm{C} \to \mathrm{C}^+ + \mathrm{e}$$

Table 1
Input parameters

Symbol	Meaning	Code Units	Note
Hydro parameters:			
n	number density of hydrogen atoms	cm^{-3}	$\rho = 1.4271 n m_H$
T	temperature	K	$T = \mu m_H P/(\rho k_b)$, μ is the molecular weight[a]
$\langle |dv/dr| \rangle$	the mean (absolute) velocity gradient[b]	s^{-1}	for LVG approximation in CO cooling
Radiation field strengths[c]:			
G_{PE}	photo-electric heating	G_0	$\gamma_{PE} = 1.87$
G_{CI}	radiation field for CI to C$^+$ photo-ionization	G_0	$\gamma_{CI} = 3.76$
G_{CO}	CO photo-dissociation (only dust shielding)	G_0	$\gamma_{CO} = 3.88$. Use the same γ for CI and CO?
G_{H_2}[d]	H$_2$ photo-dissociation (dust- and self- shielding)	G_0	dust shielding: $\gamma_{H_2} = 4.18$, self-shielding from Draine & Bertoldi (1996).
Other parameters:			
Z	metallicity	$Z_\odot$	the same metallicity for gas and dust $Z = Z_d = Z_g$
ξ_H	primary cosmic-ray ionization rate per H atom	s^{-1}H^{-1}	scales with star formation rate and surface density[e]

[a] $\mu = [m_{He,tot}x_{He,tot} + m_{H_2}x_{H_2} + m_H(1-x_{H_2})]/[m_H(x_{He,tot}+x_{H_2}+(1-2x_{H_2})+x_e)] = (m_{He,tot}x_{He,tot}+m_H)/[m_H(x_{He,tot}+1-x_{H_2}+x_e)] = 1.4271/(x_{He,tot}+1-x_{H_2}+x_e)$. $T = P/[nk_b(x_{He,tot}+1-x_{H_2}+x_e)]$.
[b] Averaged across the six faces of each grid cell in the simulation.
[c] For one-sided slab and only consider dust shielding, $G_i = G_0 \exp(-\gamma_i A_V) = G_0 \exp(-\sigma_i N_H)$, where $G_0 = 2.7 \times 10^{-3}$erg cm^{-2}s^{-1} is the interstellar radiation field in Draine (1978) (The spectrum from star clusters might be different?), $A_V = N_H/1.87 \times 10^{-21}$cm^{-2}, and the cross-section $\sigma_i = (\gamma_i/1.87) \times 10^{21}$ cm^{-2}.
[d] We only need to calculate G_{H_2} if we want to include heating by UV-pumping of H$_2$ (in high radiation field and low metallcitiy gas) or we want to calculate H$_2$ abundances in cloud edges including FUV photo dissociation (not necessary in most cases, since H$_2$ is considered to be affected by non-equilibrium chemistry).
[e] For the solar neighborhood, $\xi_H \approx 2 \times 10^{-16}$ s^{-1}H^{-1}. $\xi_{-16} = 0.472\frac{\Sigma_{SFR,-3}}{\Sigma_{gas}/50M_\odot pc^{-2}+1}$, $\xi_{-16} = \xi_H/10^{-16}$s^{-1}H^{-1}, $\Sigma_{SFR,-3} = \Sigma_{SFR}/10^{-3}M_\odot$kpc^{-2}Myr^{-1}.

Table 2
Chemical species

Species	Abundance calculation	Dependence
H$_2$	analytic, see Section 3.1	n, T, Z_d, ξ_H (and G_{H_2})
e$^-$	iterative, assumes $x_e = x_{H+} + x_{C+}$, see Section 3.2	x_{H_2}, n, T, Z_d, Z_g, ξ_H, G_{PE}, G_{CI}
C$^+$	analytic, see Section 3.2	x_e, x_{H_2}, n, T, Z_d, Z_g, ξ_H, G_{PE}, G_{CI}
H$^+$	analytic, see Section 3.2	x_e, x_{H_2}, x_{C+}, n, T, Z_d, ξ_H, G_{PE}
CO	analytic, see Section 3.3	x_{H_2}, x_{C+}, n, Z_d, Z_g, ξ_H, G_{CO}
HI	elemental conservation	$x_H = 1 - 2x_{H_2} - x_{H+}$
CI	elemental conservation	$x_{CI} = x_{C,tot} - x_{C+} - x_{CO}$
OI	elemental conservation	$x_{OI} = x_{O,tot} - x_{CO}$

and C$^+$ destruction by recombination (gas phase and on the grain surface) and reaction with H$_2$

$$C^+ + e \rightarrow C$$
$$C^+ + e + gr \rightarrow C + gr$$
$$C^+ + H_2 \rightarrow CH_2$$
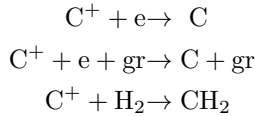
On of the main creation and destruction channels for H$^+$ is O$^+$ + H $\rightarrow$ H$^+$ + O and H$^+$ + O $\rightarrow$ O$^+$ + H. These two reactions are also the dominant channels for O$^+$ destruction and creation. The equilibrium of O$^+$ requires this two reactions to balance each other. Therefore, the H$^+$ creation and destruction from these two reactions cancel out, and we can obtain the H$^+$ abundances from the remaining important creation and destruction channels. We consider the H$^+$ creation by cosmic ray ionization and collisional ionization

$$cr + H \rightarrow H^+ + e$$
$$H + e \rightarrow H^+ + 2e$$
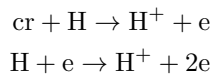
and destruction by recombination in gas phase and grain surface

$$H^+ + e \rightarrow H$$
$$H^+ + e + gr \rightarrow H + gr$$
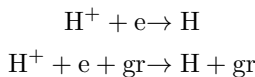
We assume most electrons comes from H$^+$ and C$^+$, which is true except for very shielded regions where the electron abundance is already very low

$$x_e = x_{H+} + x_{C+}.$$

The neutral H is calculated assuming all hydrogen is in the from of H, H$_2$ or H$^+$

$$x_H + x_{H_2} + x_{H+} = 1.$$

This is a good assumption, since the abundances of other species that contains hydrogen, H$_3^+$, H$_2^+$, CH$_x$, OH$_x$ and HCO$^+$ is very low comparing to H, H$_2$ and H$^+$.

With all the conditions above, the electron abundance can be solved iteratively. We use a iteration scheme similar to the Dekker's method (a combination of the secant method and bisection method) in root finding, and found that the electron abundance is converged within about 10 iterations. After the electron abundance is obtained, C$^+$ and H$^+$ abundance can then be calculated from the equilibrium conditions.

3.3. CO Abundance

The CO abundance is calculated making use of the fitting function Equation (25) in Gong et al. (2017):

$$\frac{n_{crit,CO}}{cm^{-3}} = \left(4 \times 10^3 Z \xi_{H,16}^{-2}\right)^{G_{CO}^{1/3}} \left(\frac{50\xi_{H,16}}{Z^{1.4}}\right), \quad (6)$$

where $n_{\rm crit,CO}$ is the critical value above which $x_{\rm CO}/x_{\rm C,tot} > 0.5$, $x_{\rm C,tot}$ the total carbon abundance, and $\xi_{\rm H,16} = \xi_{\rm H}/(10^{-16}{\rm s}^{-1}{\rm H}^{-1})$. We set the CO abundance

$$\frac{x_{\rm CO}}{x_{\rm C,tot}} = \begin{cases} 1, & n \geq 2n_{\rm crit,CO} \\ \frac{n}{2n_{\rm crit,CO}}, & n < 2n_{\rm crit,CO} \end{cases}$$

In addition, we put upper limits on the CO abundance, with $x_{\rm CO} \leq x_{\rm C,tot} - x_{\rm C^+}$ (conservation of the carbon atoms) and $x_{\rm CO}/x_{\rm C,tot} \leq 2x_{\rm H_2}$ (because H_2 is a prerequisite for CO formation).

4. HEATING AND COOLING

The heating and cooling processes included are listed in Table 3. For the details, please see Gong et al. (2017).

5. CODE TESTS

The benchmark for our model is the heating and cooling rates from equilibrium chemistry calculations in Gong et al. (2017). We also compare our results with the cooling function from Koyama & Inutsuka (2002). The comparisons below are made with unshielded (except for H_2 because of its very efficient self-shielding) gas in solar neighbourhood and low metallicity conditions: $Z = 0.1, 1$, $\xi_{\rm H} = 2 \times 10^{-16}$ s^{-1}H^{-1}, $G_{\rm PE} = G_{\rm CI} = G_{\rm CO} = 1$ (in Draine (1978) units), $G_{\rm H_2} = 0$, and $\langle |{\rm d}v/{\rm d}r| \rangle = 9 \times 10^{-14}$ s^{-1}.

The comparisons are shown in Figures 1 2. The heating and cooling rates from this work agree with that from the equilibrium chemistry in Gong et al. (2017) within a factor of ~ 2 for cold gas. The cooling rates from Wiersma et al. (2009) for hot gas agrees with that from Grackle within a factor of ~ 2. Notably, this work gives a much more accurate heating and cooling rates for cold gas than other methods. If the temperature departs from equilibrium values, the heating and cooling rates can also be very different from the heating and cooling tables from equilibrium temperatures, which is not captured by other methods (gray lines in Figure 1 and 2). However, we note that our method assumes the chemistry is always in equilibrium. Since the timescales for chemical reactions can be longer than the cooling timescales, our treatment is not completely self-consistent. To take non-equilibrium chemistry into account, one must solve the time-dependent evolution of chemical species, which will be much more computationally expensive.

6. NOTES FOR IMPLEMENTATION IN TIGRESS

1. The input parameters must be in CGS units listed in Table 1.

2. The output heating and cooling rates are in units of erg s^{-1} cm^3.

3. Because the heating and cooling rates has some steps of dividing by n, one needs to make sure that $n > 0$ (use density floor).

4. If we want to ignore the FUV dissociation of H_2 (H_2 abundance from only cosmic ray destruction, no heating from H_2 UV pumping), one just need to set $G_{\rm H_2} = 0$ in the code.

REFERENCES

Draine, B. T. 1978, ApJS, 36, 595
Draine, B. T., & Bertoldi, F. 1996, ApJ, 468, 269
Gong, M., Ostriker, E. C., & Kim, C.-G. 2018, ApJ, 858, 16
Gong, M., Ostriker, E. C., & Wolfire, M. G. 2017, ApJ, 843, 38
Hopkins, P. F., Wetzel, A., Kereš, D., et al. 2018, MNRAS, 480, 800
Kim, C.-G., & Ostriker, E. C. 2017, ApJ, 846, 133
Koyama, H., & Inutsuka, S.-i. 2002, ApJ, 564, L97
Wiersma, R. P. C., Schaye, J., & Smith, B. D. 2009, MNRAS, 393, 99

Table 3
List of Heating and Cooling Processes

Process	Dependence
Heating:	
Cosmic-ray ionization of H, H_2 and He	x_e, x_H, x_{H_2}, n, ξ_H
Photoelectric effect on dust grains	x_e, n, T, Z_d, G_{PE}
UV pumping of H_2[a]	x_H, x_{H_2}, n, T, G_{H_2}
Cooling:	
Lyα line	x_e, x_H, n, T
O fine structure line	x_e, x_{OI}, x_H, x_{H_2}, n, T
C^+ fine structure line	x_e, x_{C^+}, x_H, x_{H_2}, n, T
C fine structure line	x_e, x_{CI}, x_H, x_{H_2}, n, T
CO rotational lines	x_e, x_{CO}, x_H, x_{H_2}, n, T, $\langle|dv/dr|\rangle$
Recombination of e on PAHs	x_e, n, T, Z_d, G_{PE}
CIE cooling for hot gas[b]	T, Z_g

[a]Important at low metalicities. reference?
[b]The CIE cooling table is taken from Wiersma et al. (2009). The cooling by metals is scaled with Z_g.
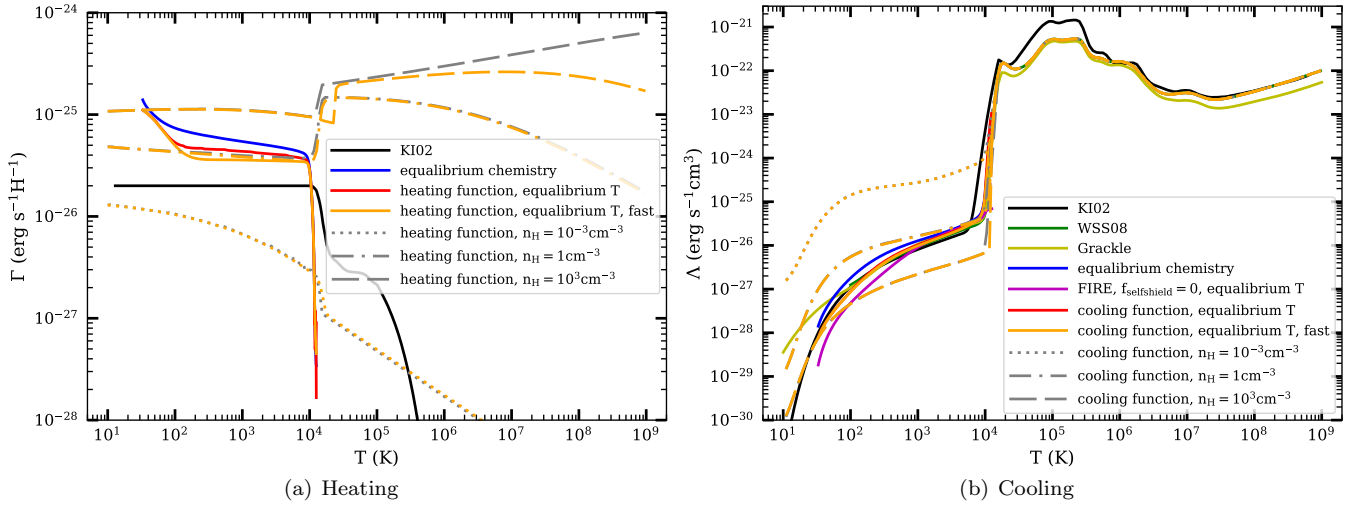

(a) Heating

(b) Cooling

Figure 1. Comparisons of heating and cooling rates for $Z = 1$. The black solid lines are the heating and cooling functions from Koyama & Inutsuka (2002) used in Kim & Ostriker (2017). The green and yellow solid lines show the cooling rates from Wiersma et al. (2009) (CIE) and Grackle (reference?). The blue solid lines are the results from equilibrium chemistry and temperature calculations by Gong et al. (2017) at densities $n = 10^{-4} - 10^3$ cm^{-3}. The equilibrium temperature from Gong et al. (2017) at different densities is shown in Figure 3. The magenta and red solid lines show the cooling (and heating for this work) rates from FIRE simulations (Hopkins et al. 2018, Equation (B18) for cold gas) and this work at these densities and equilibrium temperatures. The gray lines show the results from this work with fixed densities $n = 10^{-3}$ cm^{-3} (dotted), $n = 1$ cm^{-3} (dash-dotted), and $n = 10^3$ cm^{-3} (dashed).
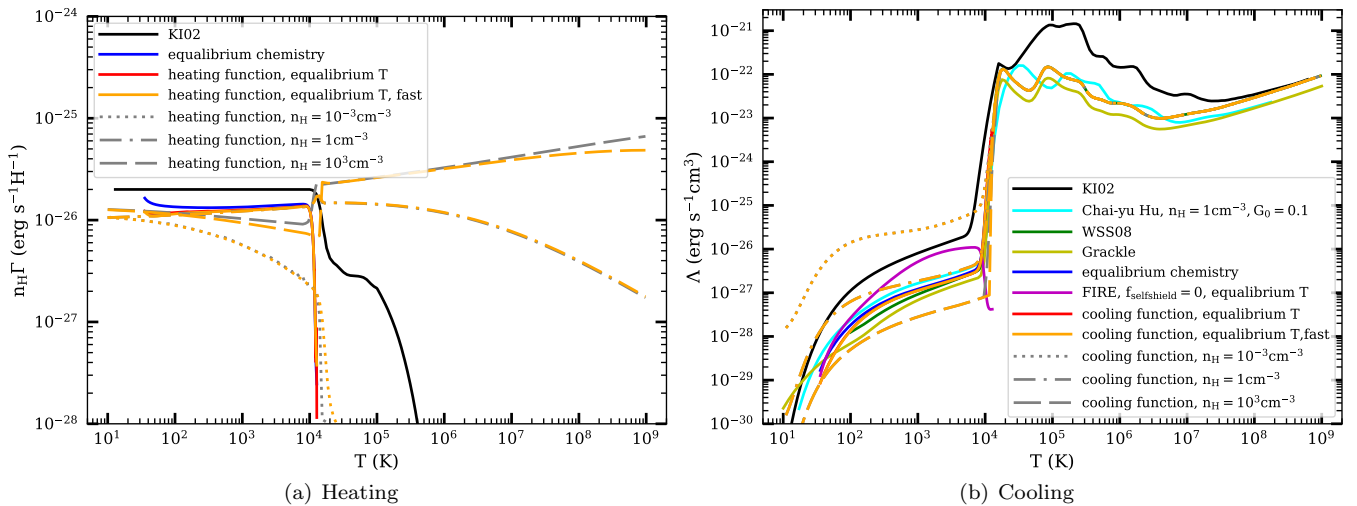

(a) Heating

(b) Cooling
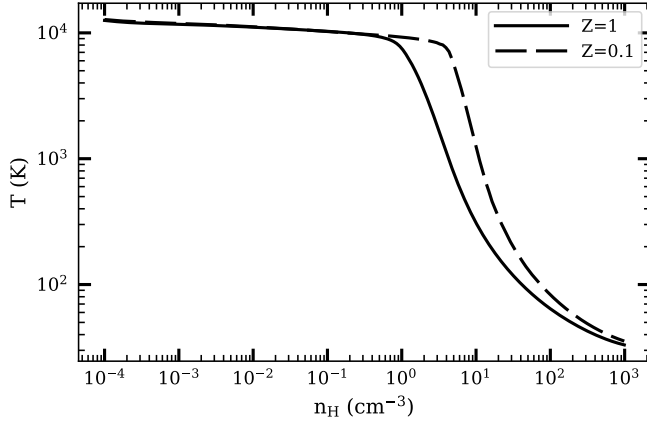
Figure 2. Similar to Figure 1, but for $Z = 0.1$.

Figure 3. Equilibrium temperature from Gong et al. (2017).